Molecular Profiling Reclassifies Adult Astroblastoma into Known and Clinically Distinct Tumor Entities with Frequent Mitogen-Activated Protein Kinase Pathway Alterations

William Boisseau, Philipp Euskirchen, Karima Mokhtari, Caroline Dehais, Mehdi Touat, Khê Hoang-Xuan, Marc Sanson, Laurent Capelle, Aurélien Nouet, Carine Karachi, et al.

Molecular profiling reclassifies adult astroblastoma into known and clinically distinct tumor entities with frequent MAPK pathway alterations

William Boisseau[1*] MD, Philipp Euskirchen[2,3,4,5,6*] MD, Karima Mokhtari[3, 7] MD, Caroline Dehais[1] MD, Mehdi Touat[3] MD, Khê Hoang-Xuan[3] MD, PhD, Marc Sanson[3] MD, PhD, Laurent Capelle[8] MD, Aurélien Nouet[8] MD, Carine Karachi[8] MD, Franck Bielle[7] MD, PhD, Justine Guégan[3] MSc, Yannick Marie[3] PhD, Nadine Martin Duverneuil[9] MD, Luc Taillandier[10] MD, PhD, Audrey Rousseau[11] MD, PhD, Jean-Yves Delattre[3] MD, Ahmed Idbaih[3] MD, PhD

* both authors contributed equally to this study

[1]AP-HP, Hôpitaux Universitaires La Pitié Salpêtrière - Charles Foix, Service de Neurologie 2-Mazarin, F-75013, Paris, France.

[2]Dept. of Neurology, Charité - Universitätsmedizin Berlin, 10117 Berlin, Germany

[3]Sorbonne Université, Inserm, CNRS, UMR S 1127, Institut du Cerveau et de la Moelle épinière, ICM, AP-HP, Hôpitaux Universitaires La Pitié Salpêtrière - Charles Foix, Service de Neurologie 2-Mazarin, F-75013, Paris, France

[4]Berlin Institute of Health (BIH), 10178 Berlin, German

[5]German Cancer Consortium (DKTK), partner site Berlin

[6]German Cancer Research Center (DKFZ), Heidelberg, Germany

[7]AP-HP, Hôpitaux Universitaires La Pitié Salpêtrière - Charles Foix, Service de Neuropathologie-Escourolle, F-75013, Paris, France.

[8]AP-HP, Hôpitaux Universitaires La Pitié Salpêtrière - Charles Foix, Service de Neurochirurgie, F-75013, Paris, France.

[9]AP-HP, Hôpitaux Universitaires La Pitié Salpêtrière - Charles Foix, Service de Neuroradiologie, F-75013, Paris, France.

[10] Dept. Of Neurology, Centre Hospitalo-Universitaire de Nancy, Nancy, France

[11]Institut Cancérologique de l'Ouest Paul Papin, 15 rue André Boquel, 49055 Angers, France

Corresponding author

Dr Ahmed Idbaih

Department of Neurology 2-Mazarin, Hôpitaux Universitaires Pitié-Salpêtrière Charles Foix, Assistance Publique Hôpitaux de Paris (APHP), Paris, France

47-83 Boulevard de l'Hôpital, 75013 Paris

Tel.: +33 1 42160385

Fax: +33 1 42160418

Email: ahmed.idbaih@aphp.fr

Keywords: astroblastoma; next-generation sequencing; *MN1-BEND2*; *BRAF* mutation

Implications for Practice:

Astroblastoma (ABM) remains a poorly defined and controversial entity. While *MN1* alterations seem to define a large subset of pediatric cases, adult cases remain molecularly poorly defined. This comprehensive molecular characterization of 1 adolescent and 14 adult ABM revealed that adult ABM histology comprises several molecularly defined entities, which explains clinical diversity and identifies actionable targets. Namely, pleomorphic xanthoastrocytoma (PXA)-like ABM case show a favorable prognosis while high-grade gliomas (glioblastoma and diffuse midline gliome)-like ABM show significantly worse clinical courses. Our results call for in-depth molecular analysis of adult gliomas with astroblastic features for diagnostic and therapeutic purposes.

Abstract

Aims and methods: astroblastoma (ABM) is a rare glial brain tumor. Recurrent MN1 alterations have been recently identified in most pediatric cases. Adolescent and adult cases, however, remain molecularly poorly defined. Here, we performed clinical and molecular characterization of a retrospective cohort of 14 adult and one adolescent ABM.

Results: Strikingly, we found that MN1 fusions are a rare event in this age group (1/15). Using methylation profiling and targeted sequencing, most cases were reclassified as either pleomorphic xanthoastrocytomas (PXA)-like or high-grade glioma (HGG)-like. PXA-like ABM show *BRAF* mutation (6/7 with V600E mutation and 1/7 with G466E mutation) and CD34 expression. Conversely, HGG-like ABM harbored specific alterations of diffuse midline glioma (2/5) or glioblastoma (3/5). These latter patients showed an unfavorable clinical course with significantly shorter overall survival ($p = 0.021$). MAPK pathway alterations (including *FGFR* fusion, *BRAF* and *NF1* mutations) were present in 10 of 15 patients and overrepresented in the HGG-like group (3/5) compared to previously reported prevalence of these alterations in GBM and diffuse midline glioma.

Conclusion: We suggest that gliomas with astroblastic features include a variety of molecularly sharply defined entities. Adult ABM harboring molecular features of PXA and HGG should be reclassified. CNS high-grade neuroepithelial tumors with *MN1* alterations and histology of ABM appear to be uncommon in adults. Astroblastic morphology in adults should thus prompt thorough molecular investigation aiming at a clear histomolecular diagnosis and identifying actionable drug targets, especially in the MAPK pathway.

Introduction

Astroblastoma (ABM) is a rare neuroepithelial tumor and has been recognized by the World Health Organization (WHO) as a distinct tumor entity.[1] It was first described in 1926 by Bailey[2] and further characterized by Bailey and Bucy[3] in 1930. ABM is generally regarded as an entity occuring in childern and young adults.[4-6] However, in a recent epidemiological survey, 56% of cases were diagnosed after 30 years of age.[7] The diagnosis of ABM is based on a typical histomorphology with perivascular astroblastic pseudorosettes and vascular hyalinization[2, 3, 8]. However, perivascular arrangement of tumor cells is not specific for ABM and may also be seen in other central nervous system tumors such as glioblastoma (GBM), primitive neuroectodermal tumors (PNET), angiocentric glioma, and ependymomas.[9, 10] The lack of specific neuropathological features explains why the validity of ABM as a distinct entity is still a matter of debate.[11]

Recently, efforts have been made to identify specific molecular alterations in ABM. In 2016, Sturm and al[12] have described a new molecularly defined tumor entity characterized by *MN1* (meningioma 1) and *BEND2* (BEN domain containing 2) fusion genes which histologically frequently corresponds to ABM. Several reports have confirmed the existence of recurrent MN1 alterations in pediatric and also adult ABM.[13-15] In contrast, Lehman and colleagues[16] showed that tumors with the histological diagnosis of ABM frequently harbor *BRAF V600E* mutations.

Here, we report a comprehensive clinical, radiological, histological and molecular characterization of a retrospective series of adolescent and adult ABM and show that they share common clinical and molecular features with other glial tumor entities.

Material and Methods

Patient cohort and histological review

Patients were retrospectively identified using systematic archival review for the term "astroblastoma" between 1990 and 2017 at the Pitié Salpêtrière university hospital, i.e. cases with (i) a final diagnosis of astroblastoma or (ii) astroblastoma being mentioned in the pathology report as a differential diagnosis. Tumors samples were stored with signed consent form in the tumor tissue bank OncoNeuroTek. All identified cases were centrally reviewed by experienced neuropathologists (KM and/or FB). Required histologic features for inclusion in the study were: (i) the presence of perivascular astroblastic pseudorosettes; (ii) the presence of hyalinized vessels; (iii) cuboidal, columnar, or tapered perivascular cellular processes, occasionally ending in broad endfeet and (iv) absence of definitive criteria for other CNS tumors. Hematoxylin and eosin staining as well as immunohistochemistry for Ki67, GFAP, IDH1 R132H, ATRX, EMA, OLIG2, vimentin, FGFR3, H3K27M, p53 and NFkB (commonly found in supratentorial ependymomas[17]) proteins were performed. Additional immunohistochemical assessment of CD34 was done post-hoc on all cases with a confirmed diagnosis of ABM.

Clinical and radiological data

For all patients, age at diagnosis, sex, clinical presentation, treatments and clinical outcome were retrospectively collected. From initial diagnosis, progression free survival (PFS) and overall survival (OS) were compared using log-rank test and plotted according to the Kaplan-Meier method.

When available, brain magnetic resonance imaging (MRI) data (T1w, T2w and contrast-enhanced T1w sequences) were reviewed and annotated for supra- vs. infratentorial location, perilesional edema, contrast enhancement, cystic component and type of tumor boundary (well defined or diffuse).

Panel DNA sequencing

All exons of genes frequently mutated in brain tumors were sequenced using a custom next-generation sequencing panel (details in **Supplementary Table 1**). Briefly, tumor DNA was extracted from FFPE or fresh-frozen tumor specimens using the QIAamp DNA mini kit (QIAGEN, Hilden, Germany) according to the manufacturer's instructions. DNA was quantified using a QuantiFluor dsDNA assay (Promega, Madison, WI, USA). Target regions were captured from fragmented genomic DNA samples using a custom SeqCap EZ choice kit (Roche NimbleGen), and paired-end 75bp massively parallel sequencing was carried out on a NextSeq500 sequencer (Illumina, San Diego, CA, USA) according to the manufacturer's protocols.

Mutation and copy number profiling

Quality control of the reads was performed with FastQC on demultiplexed data. Trimmomatic[18] was used to remove low quality segments (phred base quality < 20) of the reads at 3' and 5' ends. Reads smaller than 40 base pairs after trimming were discarded. Reads were aligned against the hg19 assembly of the human genome using BWA-MEM (version 0.7.15).[19] We then applied Genome Analysis Toolkit[20] (GATK) for base quality score recalibration and indel realignment. PatternCNV[21] was used to estimate copy number

variation based on read depth. Mutations and indels were called using GATK4 MuTect2 (beta version). SNVs were annotated using VEP.[22] Putative somatic variants were selected by filtering out all SNPs in the gnomAD release 2.0.1 with an overall population allele frequency > 0.01. [23] Variants were filtered for missense and nonsense mutations, and a minimum variant allele frequency > 0.1 was required. Disease causing variants were annotated using known cancer hotspots[24] and ClinVar.[25]

Reverse transcription PCR (RT-PCR)

First strand cDNA was generated from 500ng total RNA using Maxima First Strand Synthesis Kit (Thermo Fisher) and diluted 1:10 in molecular biology grade water. RT-PCR with primers specific for MN1-BEND2 fusions was performed using 0.02 U/µl Q5 polymerase (New England Biolabs, Ipswich, MA, USA), 200µM dNTPs, 500nM forward and reverse primers, Q5 reaction buffer with High GC Enhancer and 5µl template cDNA in total reaction volume of 20µl. Thermal cycling was performed as follows: 98°C initial denaturation for 2min, followed by 30 cycles of denaturation at 98°C for 10s, annealing at 65°C for 20s and extension at 72°C for 90s, as well as a final extension at 72°C for 2min. Amplicons were analyzed using a Caliper LabChip GX DNA 5K assay (Perkin Elmer, Waltham, MA, USA).

Quantitative realtime PCR (qPCR)

Quantitative realtime PCR of *BEND2* expression was performed in 20µl reactions using 10µl 2X LightCycler 480 SYBR Green master mix (Roche), 1µl of a 10µM forward and reverse primer mix 4µl H2O and 5µl of 1:10 prediluted cDNA. The following PCR program was used: 10min preincubation at 95°C, 45 cycles of 10s denaturation at 95°C, 10s annealing at

60°C and 10s extension at 72°C. All reactions were run in duplicates and normalized to a housekeeping gene (PPIA) using the ddCt method.

RNA sequencing and fusion gene discovery

500ng of total RNA were used for library preparation using NextSeq High Output Kit v2.5 kits (Illumina) and subjected to 2x75bp paired-end sequencing in a NextSeq 500 device (Illumina). Quality control of raw sequencing data (e.g., for potential ribosomal contamination) and insert size estimation were performed using FastQC, Picard tools, samtools and rseqc.[26] Reads were mapped using STAR v2.4.0[27] to the hg19 human genome assembly. Gene expression study was performed as described previously.[28] Briefly, for each gene present in the Human FAST DB v2016_1 annotation, reads aligning on constitutive regions (that are not prone to alternative splicing) were counted. Based on these read counts, normalization was performed using DESeq2[29] and R (v.3.2.5).

Fusion detection was performed using five different tools: Defuse v0.6.0[30], FusionCatcher v0.99.5a[31] without BLAT, JAFFA v1.06[32], SoapFuse v1.27[33], TopHat fusion v2.06.13.[34] Comparison of results between algorithms was done by FuMa v2[35] with FASTD DB v2016_1 annotations. High-confidence fusion candidates identified by > 3 tools were reviewed manually.

Methylation profiling

Genome-wide methylation profiling was performed as previously reported.[36] Briefly, 500ng of DNA were subjected to bisulfite conversion and hybridized to Infinium MethylationEPIC BeadChip microarrays (Illumina). Raw IDAT files were used as input for online methylation-

based random forest classification (www.molecularneuropathology.org) using classifier version v11b4.

Data availability

All raw sequencing data have been deposited at the European Genome-phenome Archive (accession no. EGAS00001003604). Microarray-based methylome data has been made available at ArrayExpress (accession no. E-MTAB-7490).

Results

Patients and tumors characteristics

We initially identified 25 patients with an archival diagnosis of astroblastoma (ABM). After centralized neuropathological review, a histological diagnosis of ABM was confirmed in 15 cases, 14 adults and one adolescent. Ten cases were excluded due to a morphological diagnosis of glioblastoma in seven cases, no availability of tumor DNA and RNA in two cases and co-occurrence of astroblastoma and IDH-mutant glioblastoma within the same tumor in one patient. Typical ABM histology with astroblastic pseudorosettes, perivascular pattern, vascular hyalinization and immunoreactivity for GFAP, OLIG2 and vimentin were seen in all included cases. Positive immunostaining for EMA and p53 was found in only three cases and four cases, respectively. Ten of 15 ABMs were classified as “high grade” ABM based on hypercellular zones with increased mitotic index, vascular proliferation, and necrosis.

The 15 cases included in the current study were investigated further (10 females and 5 males, sex ratio 2:1). Median age at diagnosis was 44.5 years (range: 24-66) with a bimodal age distribution: 4 patients were less than 25 years old, 7 patients more than 50 years old. The most common initial symptom was neurological deficit (8/15 patients), followed by headaches (6/15) and, seizure (4/15).

All patients underwent brain CT or MRI scan. All cases were supratentorial including one intraventricular tumor (third ventricle). Location was temporal, frontal, parietal, occipital and parieto-occipital in 6, 3, 2, 1 and 3 cases, respectively. Brain MRI was available for review in 11/15 patients. All tumors appeared well circumscribed and demarcated from normal brain on MRI. Contrast-enhancement was detected in all patients and a cystic component was observed

in 6/11 patients. All patients underwent surgical resection (13 patients with gross total resection, 2 with partial resection).

After surgery, 11 of 15 patients received adjuvant treatment (6 with combined radio- and chemotherapy, 4 with radiotherapy alone and 1 with chemotherapy alone) because of high-grade morphology (10 cases) or partial resection (1 case).

After first line treatment, 8 patients did not experience tumor relapse. In contrast 2, 4 and 1 patients experienced one, two and three or more tumors relapses, respectively. Four patients died during the follow-up period (26.7%). The median progression free survival and overall survival were 1.6 and 4.9 years respectively.

Molecular profiling

Depending on DNA and RNA availability, quantity and quality, molecular profiling was performed. Targeted next-generation panel sequencing was performed in all 15 patients, transcriptome sequencing in 4 samples and methylation profiling in 6 cases.

Together with immunohistochemistry, molecular profiling allowed the reclassification of cases into three main groups (**Figure 1A**):

ABM with molecular features of pleomorphic xanthoastrocytoma (PXA)

Seven out of 15 tumors (47%) were either classified as PXA using methylation-based classification or showed *BRAF* mutation with concomitant *CDKN2A* loss and/or immunohistochemical CD34 expression. Six tumors harbored a *BRAFV600E* mutation, which was associated with *CDKN2A* homozygous deletion in five cases and *TERT C228T* promoter mutations in 4 cases.

One patient's tumor harbored a *BRAF G466E* alteration, a class III mutation resulting in a kinase-dead form of BRAF.[37] This alteration was accompanied by a truncating NF1 mutation, a combination which is frequently observed in melanoma and known to result in a mechanistically different, yet functionally similar ERK pathway activation.[38]

None of these cases harbored typical histological features of PXA (i.e., cellular pleomorphism with spindle cells, mononucleated and multinucleated giant cells, granular bodies or positive reticulin staining).[39] Using immunohistochemistry, these cases harbored nuclear OLIG2 in all cases and cytoplasmic CD34 expression in 5/7 patients (while only 2/8 cases without *BRAF* mutation expressed CD34). Mean age at diagnosis was 25 years (**Figure 1B**). In this subgroup, one patient out of seven died during follow-up (**Figure 1C**). The median progression free survival was 2.6 years.

ABM with molecular patterns of high grade glioma (HGG)

Five out of 15 patients were classified as high-grade glioma due to presence of *H3.3 K27M* mutations or glioblastoma molecular features (methylation class GBM or any two of the following criteria: combined chr7 gain/chr10 loss, *EGFR* amplification and/or *TERT* promoter mutation).[40] Three patients had *TERT C228T* promoter mutations, one of which harbored a *FGFR3:TACC3* fusion. Interestingly, the two cases with molecular pattern of diffuse midline glioma (i.e. combination of *H3F3A*, *PPM1D* and *NF1* mutations) did not arise within classic midline location (i.e. thalamus, pons and spinal cord[41]): one case was located in the third ventricle and the other one in frontoparietal parasagittal localization. Of note, none of the H3F3A-wildtype cases in this group showed loss of histone H3 lysine 27 trimethylation.

Mean age at diagnosis in this group was 52 years (**Figure 1B**). Strikingly, this subgroup was associated with poor clinical outcome compared to PXA-like cases: three out of five patients (60%) died during the follow-up. The median progression free survival and overall survival were 0.9 and 1.9 years, respectively (**Figure 1C**).

In contrast to PXA-like cases, MR imaging of HGG-like cases showed moderate to diffuse peripheral edema with a median volume of 23.5 mL (18.8-90) vs 2.7 mL (0.7-129) in PXA-like subgroup ($p < 0.001$) (**Figure 2**).

ABM with MN1-BEND2 fusion

Only one young patient (15 years old) was epigenetically classified as high grade neuroepithelial tumour with *MN1* alteration (CNS HGNET-MN1).[12] RNA sequencing identified a *MN1:BEND2* fusion, which could be confirmed by RT-PCR and *BEND2* expression by realtime PCR while all others cases did not express BEND2 (**Supplementary Figure 1**). The patient has had stable disease since tumor resection over 19 years of follow-up.

Finally, two patients could not be assigned to either subgroup given the available molecular data. One patient (lost during follow-up) harbored a *NF1* mutation and combined chr7 gain/chr10 loss. However, because this patient did not harbor EGFR amplification, this case may correspond to PXA or GBM-like ABM.[42] The other patient harbored *CDKN2A* homozygous deletion and was positive for CD34 expression immunohistochemically.

Discussion

In this study, we retrospectively characterized a series of 14 adults and 1 adolescent with centrally reviewed ABM. The present cohort shares characteristics with previous published studies[4-6, 9, 43-46] with ABM being a supratentorial tumor with a clear female predominance and heterogeneous clinical courses. Comprehensive interrogation of genetic alterations in these 15 patients (including methylation profiling, targeted DNA sequencing, RNA sequencing, RT-PCR and qPCR) allowed re-classification of cases in three subgroups (PXA-like ABM, HGG-like ABM, and ABM with MN1-BEND2 fusion) with distinct radiological and histological features as well as clinical outcomes.

These last years, ABM has been controversial as some literature supports it as true entity with frequent MN1 alterations[12, 13, 15] while other studies suggest it does not exist as an established and unique tumor entity but could overlap with other well known tumors.[11, 14, 16, 47]
Especially, in accordance with our study, gliomas with astroblastic features may harbor molecular signature of pleomorphic xanthoastrocytoma (PXA) (ABM PXA-like) [14-16] and high grade glioma (HGG) (ABM HGG-like).[11, **14,** 47] Moreover, reclassification of ABM into more specific molecularly defined entity could explain the clinical unpredictability and difficulty in grading these tumors.

The largest group was ABM with a molecular signature of PXA. Previously, methylation-based reclassification of an ABM case into PXA-like[14, 15] and high prevalence of *BRAF* mutations[15, 16] have been reported. *BRAF* mutations are also frequently observed in gangliоglioma (GG) and pilocytic astrocytoma (PA). However, combined *BRAF V600E* mutation with (i) *CDKN2A* loss, usually only seen in PXA[48], (ii) *TERT* promoter mutations, common in anaplastic PXA, but virtually never seen in PA and rare in GG[49, 50], and (iii) positive CD34 staining demonstrates compelling evidence that indeed many ABM share the molecular identity of PXA.

The second group includes ABM with molecular features of high-grade gliomas (HGG) (i.e. GBM and diffuse midline glioma, *K27M*-mutant). As expected, these patients experienced an unfavorable clinical course. These tumors were accompanied by larger perifocal edema, a typical feature of high-grade glioma. It is interesting to note that MAPK pathway alterations including *BRAF* mutation, *NF1* mutation or *FGFR* fusion were present in 67% of cases (10/15) in the entire cohort. Even though MAPK pathway alterations are frequent in GBM (mostly affecting EGFR), they rarely involve *BRAF*, *NF1* and *FGFR*.[51, 52] Rather, the mutational spectrum resembles that of pilocytic astrocytomas.[53] Strikingly, these alterations are actionable drug targets, potentially subject to BRAF inhibition (e.g. vemurafenib), MEK inhibition (e.g. trametinib), or FGFR inhibition (e.g. NCT02052778). In addition to *BRAF* mutations, a *NRAS* mutation has previously been reported in a case of ABM,[14] extending the spectrum of observed MAPK/RAS pathway mutations. Because all of these alterations were identified retrospectively, none of the reported patients received targeted therapy.

Despite thorough multi-modal screening for MN1 alterations, only one adolescent patient was assigned the diagnosis of CNS high-grade neuroepithelial tumor with MN1 alteration. This

result differs from three previous studies in adults ABM[13-15] where MN1 rearrangements were frequent. Of note, we cannot entirely rule out MN1 alterations with fusion partners other than BEND2 in tumors that only were screened by RT-PCR and for BEND2 expression and did not undergo methylation profiling (six cases). However, all of these cases harbored glioblastoma molecular features, a *BRAF* or *H3.3 K27M* mutation and could thus reliably be assigned to one of the other subgroups. This finding is in line with evidence of previous studies, where MN1 alterations, BRAF mutation and HGG molecular features were mutually exclusive.[12-15, 47]

Our results differ partly from those of five other retrospective studies.[12-15, 47] Comparing our results directly to these studies is not possible as we encounter major differences in study population (majority of adult patients in our study versus a significant proportion of paediatric cases in others)[12-15], required histologic features, number of patients and molecular analyses performed. However, analysis of available data (summarized in Table 2) suggests that ABM with MN1 alterations appears to be frequent in children (found in 29/41 (70.7%) pediatric ABM cases) and uncommon in adults (found in 6/44 (13,6%)). In contrast, ABM with molecular features of PXA (*i.e. BRAF* mutation, CD34 expression, corresponding methylation class) appears to be recurrent in adolescent and adult (found in 14/44 (31.8%)) and rare in children (1/41 (2.4%)). Finally, most of these studies did not specifically investigate molecular features of high-grade glioma (chr7 gain/chr 10 loss, histone mutation, methylation-based classification)) and could explain why the majority of these cases (5/7) are found in our study. Additional studies with a focus on this issue would be necessary to further explore this entity.

Our study has several limitations inherent to its retrospective observational design. The diagnosis of ABM is based on fairly exclusive histologic features. This could lead to differences in patient selection and also explain differences in results between studies. Survival data should be interpreted with caution considering the three patients lost to follow-up and the study inclusion period (from 1990 to 2017): we cannot exclude the possibility that the evolution of imaging and histopathology techniques along with treatments of patients (including surgery techniques, chemotherapy and radiotherapy protocols) during the study period may have influenced our results. Finally, due to lack of material, methylation profiling could not be performed in all cases. Thus, we cannot prove that all BRAF-mutant, CD34-positive cases are indeed PXAs. Ganglioglioma, for example, remains a differential diagnosis.

In summary, our data indicate that adult ABM comprises several molecularly defined entities. CNS high-grade neuroepithelial tumor with MN1 alteration appears to be uncommon in adults. Adults' ABM frequently harbor molecular features of PXA and HGG. Astroblastic morphology in adults should prompt thorough molecular investigation aiming at a clear histomolecular diagnosis and identifying actionable drug targets, especially in MAPK pathway genes.

Acknowledgements

The authors are indebted to Amithys Rahimian-Aghda, Marine Giry, Inès Detrait and Yohann Schmitt for biobanking, sequencing studies and expert technical assistance. We would also like to thank Noémie Robil and Pierre de la Grange for fusion gene analysis, David Capper for methylation profiling, and Jean-François Côté for providing human testis tissue. PE is a participant of the BIH-Charité Clinician Scientist Program funded by the Charité - Universitätsmedizin Berlin and the Berlin Institute of Health.

Author contributions

Conception/design: William Boisseau, Philipp Euskirchen, Karima Mokhtari, Ahmed Idbaih

Provision of study material or patients: Philipp Euskirchen, Karima Mokhtari, Caroline Dehais, Khê Hoang-Xuan, Marc Sanson, Laurent Capelle, Aurélien Nouet, Carine Karachi, Franck Bielle, Justine Guégan, Yannick Marie, Nadine Martin Duverneuil, Luc Taillandier, Audrey Rousseau, Jean-Yves Delattre, Ahmed Idbaih,

Collection and/or assembly of the data: William Boisseau, Philipp Euskirchen, Karima Mokhtari, Ahmed Idbaih

Data analysis and interpretation: William Boisseau, Philipp Euskirchen, Karima Mokhtari, Ahmed Idbaih

Final approval of manuscript: William Boisseau, Philipp Euskirchen, Karima Mokhtari, Khê Hoang-Xuan, Marc Sanson, Jean-Yves Delattre, Ahmed Idbaih

Disclosures

Mehdi Touat: Agios Pharmaceutical and Taiho Oncology (C/A); **Ahmed Idbaih**: BMS, Hoffmann La Roche and Cipla (H). All other authors declared no conflict of interests.

This research was supported by a grant of the Ligue Contre le Cancer and the Institut Universitaire de Cancérologie. INCA-DGOS-Inserm_12560 SiRIC CURAMUS is financially supported by the French National Cancer Institute, the French Ministry of Solidarity and Health and Inserm. The research leading to these results has received funding from the program Investissements d'avenir (ANR-10-IAIHU-06).

References

(1) Louis DN, Perry A, Reifenberger G et al. The 2016 World Health Organization Classification of Tumors of the Central Nervous System: A Summary. *Acta Neuropathologica* 2016; 131: 803–20.

(2) Bailey P and Cushing H. *Tumors of the glioma group*. Philadelphia: Lippincott. 1924.

(3) Bailey P and Bucy PC. Astroblastomas of the brain. *Acta Psychiatr Neurol* 1930; 5: 439-461.

(4) Sughrue ME, Choi J, Rutkowski MJ et al. Clinical Features and Post-Surgical Outcome of Patients with Astroblastoma. *J. Clin Neurosci* 2011; 18: 750–54.

(5) Mallick S, Benson R, Venkatesulu B. Patterns of Care and Survival Outcomes in Patients with Astroblastoma: An Individual Patient Data Analysis of 152 Cases. *Child's Nervous System* 2017; 33: 1295–1302.

(6) Merfeld EC, Dahiya S, and Perkins SM. Patterns of Care and Treatment Outcomes of Patients with Astroblastoma: A National Cancer Database Analysis. *CNS Oncology* 2018; 7: CNS13.

(7) Ahmed KA, Allen PK, Mahajan A et al. Astroblastomas: A Surveillance, Epidemiology, and End Results (SEER)-Based Patterns of Care Analysis. *World Neurosurgery* 2014; 82: e291–97.

(8) Aldape KD, Rosenblum MK, Brat DJ. Astroblastoma. In: Louis DN, Ohgaki H, Wiestler OD, eds. WHO Classification of Tumours of the Central Nervous System, revised 4th edition. World Health Organization Classification of Tumours. Lyon, International Agency for Research on Cancer; 2016: 121-122.

(9) Brat DJ, Hirose Y, Cohen KJ et al. Astroblastoma: Clinicopathologic Features and Chromosomal Abnormalities Defined by Comparative Genomic Hybridization. *Brain Pathology* 2000; 10: 342–52.

(10) Burger PC and Scheithauer BW. Tumors of the central nervous system. Atlas of tumor pathology. Washington, DC: Armed Forces Institute of Pathology; 2007

(11) Mellai M, Piazzi A, Casalone C et al. Astroblastoma: Beside Being a Tumor Entity, an Occasional Phenotype of Astrocytic Gliomas?. *OncoTargets and Therapy* 2015; 8: 451–60.

(12) Sturm D, Orr BA, Toprak UH et al. New Brain Tumor Entities Emerge from Molecular Classification of CNS-PNETs. *Cell* 2016 ; 164: 1060–72.

(13) Hirose T, Nobusawa S, Sugiyama K et al. Astroblastoma: A Distinct Tumor Entity Characterized by Alterations of the X Chromosome and MN1 Rearrangement. *Brain Pathology* 2018. ; 28 : 684-694.

(14) Wood MD, Tihan T, Perry A et al. Multimodal Molecular Analysis of Astroblastoma Enables Reclassification of Most Cases into More Specific Molecular Entities. *Brain Pathology* 2018; 28: 192–202.

(15) Lehman NL, Usubalieva A, Lin T et al. Genomic analysis demonstrates that histologically-defined astroblastomas are molecularly heterogeneous and that tumors with MN1 rearrangement exhibit the most favorable prognosis. *Acta Neuropathol Commun* 2019 ; 7 :42

(16) Lehman NL, Hattab EM, Mobley BC et al. Morphological and Molecular Features of Astroblastoma, Including BRAFV600E Mutations, Suggest an Ontological Relationship to Other Cortical-Based Gliomas of Children and Young Adults. *Neuro-Oncology* 2016 ; 19: 31–42.

(17) Parker M, Mohankumar KM, Punchihewa C et al. C11orf95-RELA Fusions Drive Oncogenic NF-κB Signalling in Ependymoma. *Nature* 2014; 506: 451–55.

(18) Bolger AM, Lohse M and Usadel B. Trimmomatic: A Flexible Trimmer for Illumina Sequence Data. *Bioinformatics* 2014 ; 30: 2114–20.

(19) Li H. and Durbin R. Fast and accurate short read alignment with Burrows-Wheeler Transform. *Bioinformatics* 2009; 25: 1754-60

(20) McKenna A, Hanna M, Banks E et al. The Genome Analysis Toolkit: A MapReduce Framework for Analyzing next-Generation DNA Sequencing Data. *Genome Research* 2010; 20: 1297–1303.

(21) Wang C, Evans JM, Bhagwate AV et al. PatternCNV: A Versatile Tool for Detecting Copy Number Changes from Exome Sequencing Data. *Bioinformatics* 2014; 30: 2678–80.

(22) McLaren W, Gil L, Hunt SE et al. The Ensembl Variant Effect Predictor**.** *Genome Biology* 2016; 17:122.

(23) Lek M, Karczewski KJ, Minikel EV et al. Analysis of Protein-Coding Genetic Variation in 60,706 Humans. *Nature* 2016; 536: 285–91.

(24) Chang MT, Asthana, S, Gao SP et al. Identifying recurrent mutations in cancer reveals widespread lineage diversity and mutational specificity. *Nat. Biotechnol* 2016; 34:155–163

(25) Landrum MJ, Lee JM, Benson M et al. ClinVar: public archive of interpretations of clinically relevant variants. Nucleic Acids Res 2016 ; 44:D862-868.

(26) Wang L, Wang S, and Wei L. RSeQC: Quality Control of RNA-Seq Experiments. *Bioinformatics* 2012; 28: 2184–85.

(27) Dobin A, Davis CA, Schlesinger F et al. STAR: ultrafast universal RNA-seq aligner. *Bioinformatics* 2013; 29:15-21.

(28) Noli L, Capalbo A, Ogilvie C et al. Discordant Growth of Monozygotic Twins Starts at the Blastocyst Stage: A Case Study. *Stem Cell Reports* 2015. 5 : 946–53.

(29) Love MI, Huber W and Anders S. Moderated Estimation of Fold Change and Dispersion for RNA-Seq Data with DESeq2. *Genome Biology* 2014. 15: 550.

(30) McPherson A, Hormozdiari F, Zayed A et al. deFuse: An Algorithm for Gene Fusion Discovery in Tumor RNA-Seq Data. *PLoS Computational Biology* 2011 ; 7: e1001138.

(31) Nicorici D, Satalan M, Edgren H et al. FusionCatcher - a Tool for Finding Somatic Fusion Genes in Paired-End RNA-Sequencing Data. *bioRxiv* 2014 ; 011650.

(22) Davidson NM, Majewski IJ and Oshlack A. JAFFA: High Sensitivity Transcriptome-Focused Fusion Gene Detection. *Genome Medicine* 2015 ; 7: 43.

(23) Jia W, Qiu K, He M et al. SOAPfuse: An Algorithm for Identifying Fusion Transcripts from Paired-End RNA-Seq Data. *Genome Biology* 2013 ; 14 : R12.

(24) Kim D, and Salzberg SL. TopHat-Fusion: An Algorithm for Discovery of Novel Fusion Transcripts. *Genome Biology* 2011 ; 12: R72.

(25) Hoogstrate Y, Böttcher R, Hiltemann S et al. FuMa: Reporting Overlap in RNA-Seq Detected Fusion Genes. *Bioinformatics* 2016 ; 8 : 1226–28.

(26) Capper D, Jones DTW, Sill M et al. DNA Methylation-Based Classification of Central Nervous System Tumours. *Nature* 2018; 7697:469-74.

(27) Yao Z, Torres MN, Tao A et al. BRAF Mutants Evade ERK-Dependent Feedback by Different Mechanisms That Determine Their Sensitivity to Pharmacologic Inhibition. *Cancer Cell* 2015; 28: 370–83.

(28) Yao Z, Yaeger R, Rodrik-Outmezguine VS et al. Tumours with Class 3 BRAF Mutants Are Sensitive to the Inhibition of Activated RAS. *Nature* 2017; 548:234–38.

(29) Giannini C, Scheithauer BW, Burger PC et al. Pleomorphic xanthostrocytoma. What do we really know about it ? *Cancer* 1999 ; 85 :2033-2045

(30) Stichel D, Ebrahimi A, Reuss D et al. Distribution of EGFR Amplification, Combined Chromosome 7 Gain and Chromosome 10 Loss, and TERT Promoter Mutation in Brain Tumors and Their Potential for the Reclassification of IDHwt Astrocytoma to Glioblastoma. *Acta Neuropathologica.* 2018 ; 136 :793-803.

(31) Solomon DA, Wood MD, Thian T et al. Diffuse Midline Gliomas with Histone H3-K27M Mutation : a series of 47 cases assessing the Spectrum of Morphologic Variation and associated genetic alterations. *Brain Pathology* 2016 ; 5 :569-580.

(42) Brat DJ, Aldape K, Colman H et al. cIMPACT-NOW update 3: recommended diagnostic criteria for "Diffuse astrocytic glioma, IDH-wildtype, with molecular features of glioblastoma, WHO grade IV". *Acta Neuropathol* 2018 ; 136 :805-810

(43) Asha U, Mahadevan A, Sathiyabama D et al. Lack of IDH1 Mutation in Astroblastomas Suggests Putative Origin from Ependymoglial Cells? *Neuropathology* 2015; 35: 303–11.

(44) Salvati M, D'Elia A, Brogna C et al. Cerebral Astroblastoma: Analysis of Six Cases and Critical Review of Treatment Options. *J Neurooncol* 2009; 93: 369–78.

(45) Port JD, Brat DJ, Burger PC et al. Astroblastoma: Radiologic-Pathologic Correlation and Distinction from Ependymoma. *AJNR Am J Neuroradiol* 2002; 23: 243–47.

(46) Bell JW, Osborn AG, Salzman KL et al. Neuroradiologic Characteristics of Astroblastoma. *Neuroradiology* 2007; 49: 203–9.

(47) Bale TA, Abedalthagafi M, Bi WL et al. Genomic characterization of reccurent high-grade astroblastoma. *Cancer Genetics* 2016 ; 209 :321-330.

(48) Koelsche C, Sahm F, Wöhrer A et al. BRAF-Mutated Pleomorphic Xanthoastrocytoma Is Associated with Temporal Location, Reticulin Fiber Deposition and CD34 Expression. *Brain Pathology* 2014; 24: 221–29.

(49) Koelsche C, Sahm F, Capper D et al. Distribution of TERT Promoter Mutations in Pediatric and Adult Tumors of the Nervous System. *Acta Neuropathologica* 2013 ; 126:907–15.

(50) Phillips JJ, Gong H, Chen K et al. The genetic landscape of anaplastic pleomorphic xanthoastrocytoma. *Brain Pathol* 2019 ; 29 :85-96.

(51) Brennan CW, Verhaak RGW, McKenna A et al. The Somatic Genomic Landscape of Glioblastoma. *Cell* 2013 ; 155:462–77.

(52) Di Stefano AL, Fucci A, Frattini V et al. Detection, Characterization, and Inhibition of FGFR-TACC Fusions in IDH Wild-Type Glioma. *Clin Cancer Res* 2015 ; 21: 3307–17.

(53) Jones DT, Hutter B, Jäger N et al. Recurrent somatic alterations of FGFR1 and NTRK2 in pilocytic astrocytoma. *Nat Genet* 2013; 45: 927-932.

Figures legends

Figure 1. Summary of genetic alterations (A), age distribution (B) and overall survival (C) by subgroups.

Figure 2. Representative histological (A) and MRI (B) features of subgroups. (A) Hematoxylin and eosin (H&E) staining shows large astroblastic pseudorosettes in all cases (*upper panel*). Unlike HGG and HGNET-MN1, PXA-like ABM demonstrate an intense cytoplasmic and peri-cellular expression of CD34 (lower panel). (B) Representative MRI features of subgroups. Axial post-contrast T1-weighted MR images demonstrate a solid component in all cases (*upper panel*). Unlike the other subgroups, HGG-like ABM show moderate to extensive perifocal edema on FLAIR sequences (*lower panel*).

Figure 1

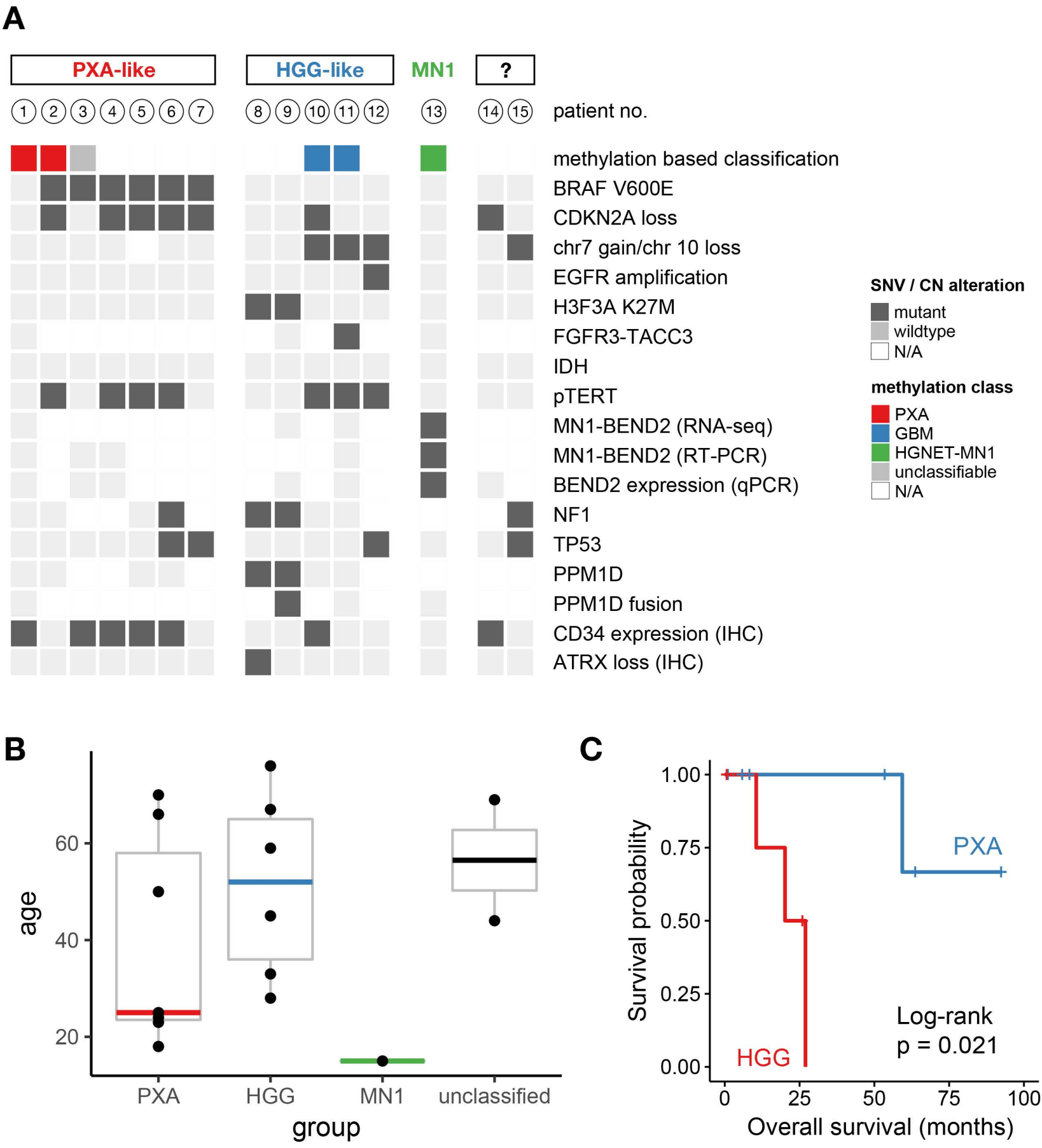
A
PXA-like
HGG-like
MN1
?
1 2 3 4 5 6 7 8 9 10 11 12 13 14 15
patient no.
methylation based classification
BRAF V600E
CDKN2A loss
chr7 gain/chr 10 loss
EGFR amplification
H3F3A K27M
FGFR3-TACC3
IDH
pTERT
MN1-BEND2 (RNA-seq)
MN1-BEND2 (RT-PCR)
BEND2 expression (qPCR)
NF1
TP53
PPM1D
PPM1D fusion
CD34 expression (IHC)
ATRX loss (IHC)
SNV / CN alteration
mutant
wildtype
N/A
methylation class
PXA
GBM
HGNET-MN1
unclassifiable
N/A
B
age
60
40
20
PXA
HGG
MN1
unclassified
group
C
Survival probability
1.00
0.75
0.50
0.25
0.00
PXA
HGG
Log-rank
p = 0.021
0
25
50
75
100
Overall survival (months)

Table 1: Patient characteristics.

	Patient no.	Age at diagnosis	Sex	Tumor location	PFS1	Treatment(s) after first surgery	Death	Overall survival (months)
PXA-like ABM	1	66	H	Parietal	1291	Surgery	No	62,7 (SD)
	2	18	H	Occipital	594	RT, CT (CCNU, bevacizumab, vemurafenib)	Yes	58,5
	3	23	F	Temporal	509	Multiple surgery	No	91,1 (SD)
	4	24	H	Temporal	1604	RT-CT then CT alone (TMZ)	No	52,7 (SD)
	5	50	F	Frontal	178	CT (TMZ)	No	5,9 (SD)
	6	70	F	Temporal	249	RT-CT (BCNU)	No	8,2 (LTFU)
	7	25	F	Frontal	30	RT-CT (TMZ)	No	1
HGG like ABM	8	45	F	Third ventricle	278	RT, CT (carboplatine, VP16)	Yes	10,4
	9	33	H	Parietal parasagittal	405	RT-CT (TMZ), Surgery, CT (Campto, bevacizumab,	Yes	26,6
	10	76	F	Parietal and Occipital	250	RT-CT (TMZ), CT (bevacizumab, BCNU)	Yes	19,9
	11	67	H	Temporal	780	No	No	25,6 (SD)
	12	59	F	Frontal	17	RT-CT (BCNU)	No	0,6 (LTFU)
MN1-BEND2 fusion	13	15	F	Parietal and occipital	3600	Surgery	No	229 (SD)

Unclassifiable patients	14	69	F	Parietal and occipital	193	RT-CT (VP-16, carboplatin)	No	**6,3 (LTFU)**
	15	44	F	Temporal	467	RT	No	**15,4 (SD)**

PFS1, progression-free survival until first recurrence, *SD*, stable disease; *LTFU*, lost to follow up; *CT*, chemotherapy; *RT*, radiotherapy; *TMZ*, temozolomide; *N/A*, not available; *PXA*, pleomorphic xanthoastrocytoma; *HGG*, high-grade glioma.

Reference	Number of patients with ABM	Number of adult cases	Number of pediatric cases	Number of cases with PXA features (BRAF mutation)	Number of cases with MN1 rearrangement	Number of cases with HGG features
This study	15	14	1	7	1 (none in adult case)	5
Sturm et al.[12]	23	0	23	?	16 (none in adult cases)	?
Bale et al.[47]	4	4	0	0$	?	1
Hirose et al.[13]	8	4	4	0*	4 (2 in adult cases)	?
Wood et al.[14]	8	6	2	1	4 (2 in adult cases)	1
Lehman et al.[15]	27	16	11	7 (1 in pediatric case)	10 (2 in adult cases)	?
Total	85	44	41	15 (1 in pediatric case)	35 (6 in adult cases)	7

Table 2 : review of litterature

- 3/8 cases were tested for BRAF mutation

$ 4/4 cases were tested for BRAF mutation